The Dust Properties of Two Hot R Coronae Borealis Stars and a Wolf-Rayet Central Star of a Planetary Nebula: in Search of a Possible Link

Geoffrey C. Clayton[1], O. De Marco[2], B. A. Whitney[3,4], B. Babler[4], J. S. Gallagher[1,5], J. Nordhaus[6], A.K. Speck[7], M.J. Wolff[3], W.R. Freeman[1], K.A. Camp[1], W.A. Lawson[8], J. Roman-Duval[9], K. A. Misselt[10], M. Meade[4], G. Sonneborn[11], M. Matsuura[12,13], and M. Meixner[9]

ABSTRACT

We present new Spitzer/IRS spectra of two hot R Coronae Borealis (RCB) stars, one in the Galaxy,V348 Sgr, and one lying in the Large Magellanic Cloud, HV 2671. These two objects may constitute a link between the RCB stars and the late Wolf-Rayet ([WCL]) class of central stars of planetary nebula (CSPNe) such as CPD –56º 8032 that has little or no hydrogen in their atmospheres. HV 2671 and V348 Sgr are members of a rare subclass that has significantly higher effective temperatures than most RCB stars, but sharing the traits of hydrogen deficiency and dust formation that define the cooler RCB stars. The [WC] CSPNe star, CPD –56º 8032, displays evidence for dual-dust chemistry showing both PAHs and crystalline silicates in its mid-IR spectrum. HV

[1]Department of Physics & Astronomy, Louisiana State University, Baton Rouge, LA 70803; gclayton@fenway.phys.lsu.edu, wfreem2@lsu.edu, kcamp5@tigers.lsu.edu

[2]Department of Physics, Macquarie University, Sydney, NSW 2109, Australia; orsola@science.mq.edu.au

[3]Space Science Institute, 4750 Walnut St. Suite 205, Boulder, CO 80301, USA; bwhitney, mjwolff@spacescience.org

[4]Department of Astronomy, 475 North Charter St., University of Wisconsin, Madison, WI 53706, USA; brian, meade@astro.wisc.edu

[5]Department of Mathematics, Physics, & Computer Science, Raymond Walters College, University of Cincinnati, Blue Ash, OH 45236; gallagjl@ucmail.uc.edu

[6]Department of Astrophysical Sciences, 116 Peyton Hall, Princeton University, Princeton, NJ 08544; nordhaus@astro.princeton.edu

[7]Physics & Astronomy, University of Missouri, Columbia, MO 65211; speckan@missouri.edu

[8]School of PEMS, University of New South Wales, Australian Defence Force Academy, P.O. Box 7916, Canberra 2610, Australia; w.lawson@adfa.edu.au

[9]STScI, 3700 San Martin Dr., Baltimore, MD 21218; duval, meixner@stsci.edu

[10]Steward Observatory, University of Arizona, 933 North Cherry Ave., Tucson, AZ 85721, USA; misselt@as.arizona.edu

[11]Observational Cosmology Laboratory Code 665, NASA Goddard Space Flight Center, Greenbelt, MD 20771, USA; george.sonneborn-1@nasa.gov

[12]Department of Physics and Astronomy, University College London, Gower Street, London WC1E 6BT, UK; mikako.matsuura@ucl.ac.uk

[13]MSSL, University College London, Holmbury St. Mary, Dorking, Surrey RH5 6NT, UK

2671 shows strong PAH emission but shows no sign of having crystalline silicates. The spectrum of V348 Sgr is very different from those of CPD –56° 8032 and HV 2671. The PAH emission seen strongly in the other two stars is not present. Instead, the spectrum is dominated by a broad emission centered at about 8.2 μm. This feature is not identified with either PAHs or silicates. Several other cool RCB stars, novae and post-asymptotic giant branch stars show similar features in their IR spectra. The mid-IR spectrum of CPD –56° 8032 shows emission features that may be associated with C_{60}. The other two stars do not show evidence for C_{60}. The different nature of the dust around these stars does not help us in establishing further links that may indicate a common origin.

HV 2671 has also been detected by Herschel/PACS and SPIRE. V348 Sgr and CPD –56° 8032 have been detected by AKARI/FIS. These data were combined with Spitzer, IRAS, 2MASS and other photometry to produce their spectral energy distributions from the visible to the far-IR. Monte Carlo radiative transfer modeling was used to study the circumstellar dust around these stars. HV 2671 and CPD –56° 8032 require both a flared inner disk with warm dust and an extended diffuse envelope with cold dust to to fit their SEDs. The SED of V348 Sgr can be fit with a much smaller disk and envelope. The cold dust in the extended diffuse envelopes inferred around HV 2671 and CPD –56° 8032 may consist of interstellar medium swept up during mass-loss episodes.

Subject headings: dust

1. Introduction

The R Coronae Borealis (RCB) stars are an extremely small class of variables, notable for their hydrogen deficiency and large irregular brightness variations caused by circumstellar dust formation (Lambert & Rao 1994; Clayton 1996). Several evolutionary scenarios have been suggested, including a merger of two white dwarfs, and a final helium shell flash (e.g., Webbink 1984; Clayton et al. 2007). RCBs are mostly made of helium. This fact and the recent detection of a high $^{18}O/^{16}O$ ratio has significantly tilted the body of evidence towards a binary merger interpretation for these stars (Asplund et al. 2000; Clayton et al. 2005, 2007; García-Hernández et al. 2009, 2010a).

Most RCB stars resemble F- or G-type supergiants. However, there is also an even rarer subclass of the RCB stars that has significantly higher effective temperatures ($\sim$15,000-20,000 K), but shares the traits of hydrogen deficiency and dust formation (De Marco et al. 2002b). Only three such stars, V348 Sgr, MV Sgr and DY Cen are known in the Galaxy. Recently, one additional star, HV 2671, was discovered in the Large Magellanic Cloud (LMC; Alcock et al. 1996; De Marco et al. 2002b). Although these four stars are part of a subclass referred to as the hot RCB stars, they do not necessarily share a common evolution (De Marco et al. 2002b). Both DY Cen and MV Sgr have typical RCB helium abundances ($\sim$98%), which exclude any currently known post-asymptotic

giant branch (post-AGB) evolutionary models, and once again support a binary merger origin for these stars (Asplund et al. 2000; Clayton et al. 2005, 2007; García-Hernández et al. 2009, 2010a). Observations of the other two hot RCB stars, V348 Sgr and HV 2671, on the other hand, lead to stellar abundance determinations that are more in line with those of Wolf-Rayet [WC] central stars of planetary nebulae (CSPN; He=40-50%, C=40-50%, O=5-10%, by mass; Herwig 2000; De Marco & Barlow 2001; De Marco et al. 2002b).

While the abundances of V348 Sgr have been determined by Leuenhagen & Hamann (1994), the abundances of HV 2671 have not, but its low-resolution spectrum is almost identical to that of V348 Sgr. The visible spectra of V348 Sgr and HV 2671, as well as their abundances, are similar to those of the [WC10] CPD –56º 8032 (De Marco & Crowther 1998; De Marco et al. 2002b). However, both V348 Sgr and HV 2671 are cooler (∼20,000 K) than the [WC10] spectral class (∼34,000 K) (Leuenhagen & Hamann 1994; De Marco & Crowther 1998), such that Crowther et al. (1998) suggested that V348 Sgr fails the late Wolf-Rayet ([WCL]) criterion altogether. Wolf-Rayet CSPN have been explained as stars such as V605 Aql that suffer a last helium shell flash just before or after the departure of the stars from the AGB (e.g., Herwig 2001; Clayton et al. 2006). However, several of their observed characteristics are not explained by this model and this has invited alternative, binary-based scenarios (e.g., De Marco & Soker 2002; De Marco 2008)

All of the stars are hydrogen deficient but the amount of hydrogen present varies greatly from star to star (De Marco et al. 2002b). V348 Sgr has a measured hydrogen abundance of 4% by mass but this may be an upper limit. HV 2671 has no measurement of its hydrogen abundance but its spectrum looks very similar to that of V348 Sgr. The hydrogen abundance by mass in CPD –56º 8032 is <1% (De Marco & Crowther 1998). The hot RCB stars, V348 Sgr and HV 2671, as well as the [WC10] CPD –56º 8032 are surrounded by hydrogen-rich PNe: there is a large PN (∼30″) observed around V348 Sgr (Pollacco et al. 1991), and a young, dense PN is seen around CPD –56º 8032 (De Marco et al. 1997). HV 2671 likely has a PN also (De Marco et al. 2002b), as can be inferred by its Balmer and [O III] emission lines. However, HV 2671 shows no sign of extended Hα emission on images obtained for the Reid-Parker LMC PN survey (Reid & Parker 2006a,b), likely due to its large distance.

The lightcurve behavior of HV 2671 and V348 Sgr is typical for RCB stars with periods of inactivity followed by sudden declines in brightness by several magnitudes and slow returns to maximum light (Alcock et al. 1996; Alcock et al. 2001; De Marco et al. 2002b; Soszyński et al. 2009). V348 Sgr, in particular, is very active, showing many declines of 4 mag or more. The declines seen in CPD –56º 8032 are similar in form to those seen in RCB stars although they are much shallower (∼1 mag) (Jones et al. 1999; Cohen et al. 2002). The CPD –56º 8032 declines have been associated with an obscuring disk resolved with HST and VLTI (De Marco et al. 2002a; Chesneau et al. 2006). No such high spatial resolution observations exist for V348 Sgr and HV 2671.

The link between RCB and [WC] CSPN may reside in a binary interaction that generated

both classes. As pointed out previously, there is now compelling evidence that the RCB stars were produced in a merger of two WDs. [WC] stars, on the other hand, have abundances consistent with post-AGB single star evolution. However, one line of evidence that undermines this interpretation derives from the observations of circumstellar dust. Cohen et al. (1989) found that CPD –56º 8032 shows the emission features ascribed to polycyclic aromatic hydrocarbons (PAHs) in its IR spectrum. Its PN shows C/O>1 (De Marco et al. 1997), so it was a surprise to also find that the mid-IR spectrum of CPD –56º 8032 also shows the presence of many emission features attributed to crystalline silicates. The simultaneous presence of both C-rich and O-rich chemistry and dust (Barlow 1997; Waters et al. 1998; Cohen et al. 1999) may point to the presence of a long lived disk which may have formed through binary interaction (Waters et al. 1998; Cohen et al. 1999, 2002) and this was corroborated by the detection of an edge-on disk around this star (De Marco et al. 2002a). These findings are in line with a binary scenario for this object and possibly for the class of [WCL] CSPNe (Zijlstra 2001; De Marco & Soker 2002; De Marco 2008). It was suggested that the dual-dust chemistry phenomenon in PNe seems showed a strong correlation with the presence of a late [WC] nucleus (Cohen et al. 2002), but more recent Spitzer observations of the Galactic Bulge show that dual-dust chemistry is common in all (cool and hot) [WC]-type PNe (Perea-Calderón et al. 2009; Guzman-Ramirez et al. 2011). A final thermal pulse on the AGB or hydrocarbon chemistry in an UV-irradiated, dense torus may be responsible.

In this paper, we present new Spitzer/IRS spectra of HV 2671 and V348 Sgr, which have been analyzed and compared with that of CPD –56º 8032 to look for evidence for dual-dust chemistry that may establish further links between the hot RCB and [WC] classes that that may possibly elucidate the connection between the dust and the evolution that generated it. We also present the spectral energy distributions (SEDs) of the three stars from the visible to the far-IR using new Spitzer, AKARI and Herschel photometry. These SEDs have been modeled using a Monte Carlo radiative transfer (RT) code to determine the nature of the circumstellar dust around these stars and infer their mass-loss history.

2. Observations and Data Reduction

The new Spitzer/IRS spectra of HV 2671 and V348 Sgr were obtained in Stare mode as part of program 30380. The two targets were observed with the Short-Low (SL; $5.2 - 14$ μm; $\lambda/\Delta\lambda \sim 90$) and Long-Low (LL; $14 - 38$ μm; $\lambda/\Delta\lambda \sim 90$) low-resolution modules. The observations used a ramp time of 6s with 5 cycles of standard pointed observations for V348 Sgr and 10 cycles for HV 2671. So each of the bands (SL1, SL2, LL1 and LL2) was integrated for 63s for V348 Sgr and 126s for HV 2671. V348 Sgr was observed on 2006 October 22, and HV 2671 was observed on 2006 November 14.

Our point-source extraction and calibration method has been extensively employed in Furlan et al. (2006), Sargent et al. (2006), Watson et al. (2007), and Sargent et al. (2009) to which we refer the reader for more detail. We start with the SSC IRS pipeline *Basic Calibrated Data* (BCD)

product for each object. The BCD is flat-fielded, dark-current subtracted, and stray-light corrected. We employ a point-source spectral extraction and calibration method using the Spectral Modeling, Analysis and Reduction Tool (SMART; Higdon et al. 2004) and IDL routines for post-pipeline processing. In particular, we identify and correct for rogue (NaN) pixels in our two dimensional spectral data by linearly interpolating the four nearest neighboring pixel values. To correct for the sky background, we subtract the off-order spectrum ($\sim$1-3$'$ away from target) in the same nod position of the on-target order. The low-resolution sky-subtracted spectra are then extracted using a variable-width extraction window that fits tightly to the IRS point-spread function.

To calibrate our spectra, we employ custom relative spectral response functions (RSRFs) which yield flux densities based on the signal detected at a given wavelength. To produce the RSRFs, we use SMART to divide each of our spectra nod by nod for each order of each module. A spectral template of a calibration star (α Lac; Cohen et al. 2003) was identically prepared such that the quotient of the template and the observed stellar spectrum is the RSRF. The low-resolution, sky-subtracted extractions were then multiplied by the RSRF corresponding to the relevant nod, order and module. In general, we found good agreement between flux values in regions of wavelength overlap between orders in each module. For each object, the procedure described above produces a calibrated point-source spectrum. For V348 Sgr, there was a problem with the SL2 nod 1 data which caused a mismatch in the 8 μm region. So only the SL2 nod 2 data were used. The small apparent emission features seen in the 21 μm region for V348 Sgr are not real but are the result of splicing the spectra.

Figure 1 shows the fully reduced IRS spectra of V348 Sgr and HV 2671. The ISO spectrum of CPD –56º 8032 is also plotted for comparison (Cohen et al. 1999). To enhance the emission features, the underlying continua have been fitted and removed. It was not possible to fit any of the three continua with a single modified blackbody. The dust around these stars has a distribution of temperatures so a power law was used to fit the continuum of each star which was then subtracted (Guha Niyogi et al. 2011). The emission shown in Figure 1 comes from a region of $\sim$3$''$.6 and 10$''$.2 for the SL and LL modules, respectively. The ISO SWS apertures are quite large ($\geq$14$''$x 20$''$). Two ISO spectra exist for V348 Sgr but they have very low S/N (Sloan et al. 2003). They will not be considered further here. There is no sign of extended emission in the IRS spectra of HV 2671 and V348 Sgr.

In Figures 2-4, the SEDs of HV 2671, V348 Sgr and CPD –56º 8032 are plotted from the visible to the far-IR. The data, summarized in Tables 1-3, consist of visible photometry, 2MASS JHK, as well as IRAS photometry (Walker 1985; Rao & Nandy 1986). AKARI/IRC and FIS photometry are also available for the three stars (Murakami et al. 2007; Ishihara et al. 2010). For HV 2671, Spitzer and Herschel photometry are also available. The Spitzer/IRAC and MIPS 24 μm photometry were obtained from the catalogs provided by the SAGE Legacy project (Meixner et al. 2006). MIPS spectra (52-93 μm) were also obtained for HV 2671 (van Loon et al. 2010). Herschel data for HV 2671 were obtained as part of the HERITAGE Key Program (Meixner et al. 2010). Fluxes were extracted from PACS (100, 160 μm) and SPIRE (250 μm) using Starfinder (Diolaiti et al. 2000).

Starfinder produced point spread function (PSF) fitted photometry using PSFs for each instrument which were downloaded from the Herschel Science Center. No aperture corrections were applied since the PSFs used were of sufficiently large diameter. The uncertainties quoted in Table 1 and plotted in Figure 2 for PACS and SPIRE are the Starfinder uncertainties plus calibration errors of 5% for SPIRE and 10% for PACS. Figure 5 shows the HV 2671 source in the Spitzer/IRAC 8.0 μm, Spitzer/MIPS 24 μm, and SPIRE 250 μm bands. HV 2671 is also visible on the SPIRE 350 and 500 μm images but photometry was not attempted because the field is confused with diffuse emission.

3.   Dust Emission Features in the Mid-IR

The optical spectra of CPD –56º 8032, V348 Sgr, and HV 2671 can be found in De Marco & Crowther (1998), Leuenhagen et al. (1994), and De Marco et al. (2002b), respectively. The stellar spectra exhibit narrow emission lines. In the case of CPD –56º 8032 the spectrum is dominated by C IV and C III, while in the case of V348 Sgr, C IV is absent and the spectrum is dominated by neutral and singly ionized species, denoting a cooler atmosphere (Leuenhagen & Hamann 1994). The abundances of these stars, determined by non-LTE, spherical wind models are very similar indeed. Based solely on the abundances and the appearance of the stellar spectrum one would deduce that the cooler stars have left the AGB more recently and, given time, they will heat up to look more like CPD –56º 8032.

The IR spectra, however, seem to tell a different story. In Figure 1, CPD –56º 8032 clearly shows the usual PAH emission bands at 6.2, 7.7, 8.7 and 11.3 μm along with the emission "plateaus" at 6–9 and 11–14 μm (Cohen et al. 1999). The ISO spectrum also shows the 3.3 and 5.2 μm PAH features, not plotted here. The spectrum of HV 2671 mimics the features of CPD –56º 8032 very closely so that from 5 to 15 μm the spectra are close to identical. Also identified in Figure 1, are the crystalline silicate features of Enstatite and Forsterite in the CPD –56º 8032 spectrum (Cohen et al. 2002). HV 2671 shows no significant emission from crystalline silicates although it may show the same unidentified emission feature at 32.8 μm.

The spectrum of V348 Sgr is very different from those of CPD –56º 8032 and HV 2671. A continuum consisting of a 725 K blackbody and a 63 K modified blackbody was subtracted to produce the spectrum of V348 Sgr shown in Figure 1 (Lambert et al. 2001; Guha Niyogi et al. 2011). There is no PAH emission. There is a weak emission feature present at 6.4 μm. The spectrum is dominated by a broad emission centered at about 8.2 μm. This feature is not identified with either PAHs or silicates. The V348 Sgr spectrum is quite similar to the average spectrum of nine RCB stars (García-Hernández et al. 2011). The broad feature at $\sim$8 μm has been attributed to amorphous carbon (Colangeli et al. 1995) and hydrogenated amorphous carbon (Lambert et al. 2001). Nova DZ Cru shows a similar spectrum to V348 Sgr with a broad feature at 8.2 μm and no other strong features (Evans et al. 2010). The feature is attributed to hydrogenated amorphous carbon (AC) with aliphatic bands. Several other novae and post-AGB stars have shown similar

features in their IR spectra (Evans et al. 2010). The post-AGB stars fall into the Class C which has broad emission features at ∼6.3 and 8.2 μm ascribed to C-C modes (Sloan et al. 2007). The luminous transient, NGC 300-OT, also shows a similar mid-IR spectrum with a strong emission feature at ∼8.5 μm (Prieto et al. 2009). Both HV 2671 and V348 Sgr have two atomic emission lines from ionized elements, likely deriving from the PN ([Si II] at ∼34.8 μm and [S III] at ∼33.4 μm). This is evidence of a PN round HV 2671. There also is a possible Fe II line at 35.8 μm in both objects.

Recently, emission features associated with C_{60} have been identified in in several PNe (Cami et al. 2010; García-Hernández et al. 2010b), a proto-PN (Zhang & Kwok 2011), in the interstellar medium (Sellgren et al. 2010), and in the least H-deficient RCB stars, DY Cen and V854 Cen (García-Hernández et al. 2011). DY Cen is a hot RCB star like V348 Sgr and HV 2671. However, as mentioned above, the helium abundances of V348 Sgr and HV 2671 are more similar to [WC] CSPNe like CPD –56º 8032 than to the cooler RCB stars, while DY Cen's helium abundance resembles the cooler RCB stars. The C_{60} features identified in García-Hernández et al. (2011) are marked in Figure 1. The features appear at 7.0, 8.5, 17.4, and 18.9 μm. There is also a PAH feature at 8.6 μm. The spectrum of CPD –56º 8032 shows evidence of C_{60} emission. However, the other two stars show no such emission. If these are C_{60} features in CPD –56º 8032, then the 17.4 and 18.9 μm features are broader than those seen in Tc 1 but still narrower than dust grain features. They are more similar to those seen in the RCB stars, DY Cen and V854 Cen (Cami et al. 2010; García-Hernández et al. 2011). Like in V854 Cen, the 7.0 and 17.4 μm features are blended with several PAH emission features so it is not possible to measure the line ratio accurately (García-Hernández et al. 2011). But comparing the peak emissions in the 7.0/18.9, 8.5/18.9, and 17.4/18.9 ratios gives values that are consistent with the observations and predictions of C_{60} (Sellgren et al. 2010). It is interesting that C_{60} may be detected in the least hydrogen-deficient RCB stars since CPD –56º 8032, while hydrogen deficient, still has a significant hydrogen abundance (De Marco & Crowther 1998). García-Hernández et al. (2011) suggest that C_{60} may form from the decomposition of hydrogenated amorphous carbon in moderately hydrogen-deficient circumstellar shells.

In conclusion, while the dust spectrum of CPD –56º 8032, with the dual-chemistry signature, may well be indicating the presence of a disk that formed by binary action in the early AGB phase when the star was oxygen-rich, the other spectra are not obviously explained by this scenario (Cohen et al. 1999, 2002). HV 2671 is similar to CPD –56º 8032 in its dust properties, but it has no sign of silicate emission. It is possible that the silicate features are just weaker. V348 Sgr, however, is completely different. We may have expected it to be similar to HV 2671 on the grounds of their almost identical optical spectra, but it is not. Its dust emission is difficult to interpret. The resemblance of V348 Sgr to some novae establishes only one weak and circumstantial connection to this class of binaries, a connection that has been established between the [WC] spectra class and ONeMg novae on the grounds of high neon abundances found in the ejecta of the [WC] V605 Aql and two other related stars (Wesson et al. 2003, 2008; Lau et al. 2011), and between post-common envelope CSPN and novae (Rodríguez-Gil et al. 2010). A more solid link between [WC] stars,

RCBs remains elusive and the presence or absence of dual-dust chemistry is not a definitive clue to binarity.

4. Radiative Transfer Modeling of the Circumstellar Dust

A comparison of the IRAS and ISO data from the 80's and 90's with the newer Spitzer and AKARI data indicates that the mid-IR emission does not vary significantly over these timescales in any of the three stars. No significant flux variation is seen between the two IRAC/SAGE epochs for HV 2671 (Meixner et al. 2006). Previous modeling showed that the IRAS photometry for V348 Sgr can be fit with a 550 K black body (Walker 1985), but Rao & Nandy (1986) note that the near-IR and IRAS photometry cannot be fit by a single black body. The 60 μm point for V348 Sgr sits above the $\sim$600 K black body fit to the other data, and indicates the presence of a cooler dust component. Tisserand et al. (2009) suggest that the HV 2671 dust is thick and cold compared to other RCB stars based on Spitzer IRAC and MIPS colors.

The availability of photometry for the three stars from the optical to the far-IR provides an opportunity to model the radiative transfer (RT) in their circumstellar dust shells. We have modeled the SEDs of the three stars using a Monte Carlo RT code which includes nonisotropic scattering, polarization, and thermal emission from dust in a spherical-polar grid (Whitney et al. 2003a,b; Robitaille et al. 2006). All of the models were done with amorphous carbon dust and an MRN size distribution (Mathis et al. 1977). We have assumed a mass gas-to-dust ratio of 100. The best fits to the SEDs are shown in Figures 2-4. The best fitting model for all three stars consists of a flared disk surrounded by a large low-density envelope (5×10^{-21} g cm^{-3} in the outer regions, with an r^{-2} radial dependency) that includes a bipolar, lower-density cavity (1×10^{-21} g cm^{-3}). Heating by the interstellar radiation field was included but was found to be negligible. The stellar parameters and circumstellar dust parameters are summarized in Table 4, where disk and envelope masses are based on the dust mass and a gas-to-dust ratio of 100. The fits to the SEDs of HV 2671, V348 Sgr and CPD –56º 8032 are shown in Figures 2, 3 and 4, respectively. These models are not unique but do provide a general idea of the dust geometry around these stars.

The SEDs of all three sources are fit with a combination of a circumstellar disk and a more extended envelope partially evacuated in the polar regions. The disk provides mid-IR emission from warm dust near the star, the extended envelope supplies the far-IR emission from cooler dust, and the bipolar cavities allow optical radiation to escape with relatively low extinction. The envelope surrounding V348 is relatively small and optically thin. The envelopes surrounding the other two stars are much larger and more opaque, with bipolar cavities subtending 40°– 50° (Table 4). The large-scale dust may or may not be associated with the stars, as discussed below. The inner hot dust can be fitted by a disk or a patchy distribution of dust, but a complete shell would increase the extinction more than allowed by the data. A disk is consistent with the dust geometry inferred for CPD –56º 8032 by *Hubble Space Telescope* (De Marco et al. 2002a) as well as with the model of an oxygen rich disk within a carbon rich, more distributed dusty environment (Cohen et al.

1999). The geometry of the dust around the RCB stars in not certain but there is some evidence for disk-like geometries (e.g., Rao & Raveendran 1993; Clayton et al. 1997; Bright et al. 2011). A patchy distribution of dust is consistent with the production of dust in puffs in the RCB stars (Feast et al. 1997).

The best fit to the SED of V348 Sgr is not as successful as those for the other two stars. This is mainly due to the presence of the strong broad emission feature at ∼8.2 μm in the IRS spectrum of V348 Sgr which is not accounted for in the radiative transfer which models only the continuum dust emission due to amorphous carbon grains. The SED of V348 Sgr is fit with a disk and envelope like HV 2671 and CPD –56º 8032 but much smaller in extent and mass. In this sense, V348 Sgr sets itself apart from the other two objects.

The total envelope mass inferred for HV 2671 and, to a lesser extent for CPD –56º 8032, is large and would imply relatively high mass stars (We recall that the likely median progenitor mass for PN is 1.2 $M_\odot$, Moe & De Marco 2006). However, not all the mass in the low-density envelope may have come from the star itself. HV 2671 lies in an area of strong diffuse dust emission at far-IR wavelengths and it is a hot, luminous star that will heat up a large volume of low-density ISM. It should be noted that since HV 2671 is in the LMC a resolution element will sample a volume $\geq$ 1000 times greater than for the two Galactic stars. CPD –56º 8032 also needs a large diffuse envelope for its RT models. The inferred densities of these envelopes, while low, are still orders of magnitudes higher than the typical diffuse ISM, so this material may have been swept up by the material lost from these stars. Similar shells have been seen around other evolved stars including the final-flash star, V605 Aql (Young et al. 1993; Clayton & De Marco 1997). R CrB, itself, shows a very large shell seen at IRAS 100 μm (Gillett et al. 1986). That shell has a total shell mass of ∼1 $M_\odot$ and a density of 0.07 cm^{-3}. It is larger and more diffuse than the shell around HV 2671. The model shown in Figure 2 does not fit the SPIRE 250 μm point very well. We could improve the fit by placing low-density material in a shell at 5 pc radius from the star. The mass of such a large shell is enormous, 58,000 $M_\odot$. This suggests that the dust contributing to the 250 μm point is not associated with the star.

The HV 2671 dust shows no sign of silicates and is fit well by an RT model with AC dust. The dust around CPD –56º 8032, which contains both silicates and AC, is nevertheless fit extremely well by the AC only dust. Models with a mixture of silicates and AC achieve similar fits to the SED of CPD –56º 8032. This shows that the correct geometry is more important to a good fit than the dust properties.

Finally, this is the first time that we are detecting cold dust heated by these stars. Despite the very large declines in brightness (∼8 mag) seen in the RCB stars, the amount of dust responsible for each decline is small. The dust is thought to form in small clumps around the star which if along the line of sight cause a decline. These clumps are ∼10^{-8} $M_\odot$ and the mass loss rate per year is about ten times larger than that (Clayton et al. 1992; Clayton 1996). The lifetime of an RCB star is unknown but may be 10^4 to 10^5 yr (e.g., Zaniewski et al. 2005). So assuming a normal

gas-to-dust ratio, an RCB star could lose ~ 1 M$_\odot$ in its lifetime. Therefore, the large difference between the amount of gas and dust around HV 2671 and V348 Sgr may have more to do with the ISM environment of the stars, in particular since the the inner dust properties of these two stars are not dissimilar.

5. Summary

We have observed the IR spectra of two of the four hot RCB stars, V348 Sgr and its apparent twin in the LMC, HV 2671. These two objects may constitute a link between the RCB stars and the [WC] class of CSPNe that has no hydrogen in their atmospheres. We have also observed the IR spectrum of the [WC] star, CPD –56º 8032, which also shows RCB-type declines. We expected that the dust chemistries of these three stars might be similar, and reveal further links between the two classes that would elucidate their possible common ancestry. In particular, detecting the presence of dual-dust chemistry would have established a much stronger link between RCB stars and the [WC] central stars of PNe. This has not happened, however. The spectrum of HV 2671 is somewhat similar to that of CPD –56º 8032, but it lacks the strong crystalline silicate features that we ascribe to the disk of CPD –56º 8032. It could be that these features are simply weaker and that the two dusty environments are actually quite similar. On the other hand, the spectrum of V348 Sgr is completely different from those of the other two stars. This spectrum is similar to that of cool RCB stars and a handful of novae. Radiative transfer models of the three dusty environments reveal that the mass of ejected dust and gas must be quite large, in particular for HV 2671. If this massive cool envelope is not swept up interstellar gas, then these findings point to the fact that HV 2671 had a mass at the high end of the intermediate mass-spectrum.

REFERENCES

Alcock, C., et al. 1996, ApJ, 470, 583

Alcock et al. 2001, ApJ, 554, 298

Asplund, M., Gustafsson, B., Lambert, D. L., & Rao, N. K. 2000, A&A, 353, 287

Barlow, M. J. 1997, Ap&SS, 251, 15

Bright, S. N., Chesneau, O., Clayton, G. C., de Marco, O., Leão, I. C., Nordhaus, J., & Gallagher, J. S. 2011, MNRAS, 621

Cami, J., Bernard-Salas, J., Peeters, E., & Malek, S. E. 2010, Science, 329, 1180

Chesneau, O., et al. 2006, A&A, 455, 1009

Clayton, G. C. 1996, PASP, 108, 225

Clayton, G. C., Bjorkman, K. S., Nordsieck, K. H., Zellner, N. E. B., & Schulte-Ladbeck, R. E. 1997, ApJ, 476, 870

Clayton, G. C., & De Marco, O. 1997, AJ, 114, 2679

Clayton, G. C., Geballe, T. R., Herwig, F., Fryer, C., & Asplund, M. 2007, ApJ, 662, 1220

Clayton, G. C., Herwig, F., Geballe, T. R., Asplund, M., Tenenbaum, E. D., Engelbracht, C. W., & Gordon, K. D. 2005, ApJ, 623, L141

Clayton, G. C., Kerber, F., Pirzkal, N., De Marco, O., Crowther, P. A., & Fedrow, J. M. 2006, ApJ, 646, L69

Clayton, G. C., Whitney, B. A., Stanford, S. A., & Drilling, J. S. 1992, ApJ, 397, 652

Cohen, M., Barlow, M. J., Liu, X.-W., & Jones, A. F. 2002, MNRAS, 332, 879

Cohen, M., Barlow, M. J., Sylvester, R. J., Liu, X.-W., Cox, P., Lim, T., Schmitt, B., & Speck, A. K. 1999, ApJ, 513, L135

Cohen, M., Megeath, S. T., Hammersley, P. L., Martín-Luis, F., & Stauffer, J. 2003, AJ, 125, 2645

Cohen, M., Tielens, A. G. G. M., Bregman, J., Witteborn, F. C., Rank, D. M., Allamandola, L. J., Wooden, D., & Jourdain de Muizon, M. 1989, ApJ, 341, 246

Colangeli, L., Mennella, V., Palumbo, P., Rotundi, A., & Bussoletti, E. 1995, A&AS, 113, 561

Crowther, P. A., De Marco, O., & Barlow, M. J. 1998, MNRAS, 296, 367

De Marco, O. 2008, in Astronomical Society of the Pacific Conference Series, Vol. 391, Hydrogen-Deficient Stars, ed. A. Werner & T. Rauch, 209

De Marco, O., & Barlow, M. J. 2001, Ap&SS, 275, 53

De Marco, O., Barlow, M. J., & Cohen, M. 2002a, ApJ, 574, L83

De Marco, O., Barlow, M. J., & Storey, P. J. 1997, MNRAS, 292, 86

De Marco, O., Clayton, G. C., Herwig, F., Pollacco, D. L., Clark, J. S., & Kilkenny, D. 2002b, AJ, 123, 3387

De Marco, O., & Crowther, P. A. 1998, MNRAS, 296, 419

De Marco, O., & Soker, N. 2002, PASP, 114, 602

Diolaiti, E., Bendinelli, O., Bonaccini, D., Close, L., Currie, D., & Parmeggiani, G. 2000, A&AS, 147, 335

Evans, A., et al. 2010, MNRAS, 406, L85

Feast, M. W., Carter, B. S., Roberts, G., Marang, F., & Catchpole, R. M. 1997, MNRAS, 285, 317

Furlan, E., et al. 2006, ApJS, 165, 568

García-Hernández, D. A., Hinkle, K. H., Lambert, D. L., & Eriksson, K. 2009, ApJ, 696, 1733

García-Hernández, D. A., Kameswara Rao, N., & Lambert, D. L. 2011, ApJ, 729, 126

García-Hernández, D. A., Lambert, D. L., Kameswara Rao, N., Hinkle, K. H., & Eriksson, K. 2010a, ApJ, 714, 144

García-Hernández, D. A., Manchado, A., García-Lario, P., Stanghellini, L., Villaver, E., Shaw, R. A., Szczerba, R., & Perea-Calderón, J. V. 2010b, ApJ, 724, L39

Gillett, F. C., Backman, D. E., Beichman, C., & Neugebauer, G. 1986, ApJ, 310, 842

Guha Niyogi, S., Speck, A. K., & Onaka, T. 2011, ApJ, 733, 93

Guzman-Ramirez, L., Zijlstra, A. A., Níchuimín, R., Gesicki, K., Lagadec, E., Millar, T. J., & Woods, P. M. 2011, MNRAS, 441

Heck, A., Houziaux, L., Manfroid, J., Jones, D. H. P., & Andrews, P. J. 1985, A&AS, 61, 375

Herwig, F. 2000, A&A, 360, 952

—. 2001, ApJ, 554, L71

Higdon, S. J. U., et al. 2004, PASP, 116, 975

Ishihara, D., et al. 2010, A&A, 514, A1

Jones, A., Lawson, W., De Marco, O., Kilkenny, D., van Wyk, F., & Roberts, G. 1999, The Observatory, 119, 76

Lambert, D. L., & Rao, N. K. 1994, Journal of Astrophysics and Astronomy, 15, 47

Lambert, D. L., Rao, N. K., Pandey, G., & Ivans, I. I. 2001, ApJ, 555, 925

Lau, H. H. B., de Marco, O., & Liu, X. 2011, MNRAS, 410, 1870

Leuenhagen, U., & Hamann, W. 1994, A&A, 283, 567

Leuenhagen, U., Heber, U., & Jeffery, C. S. 1994, A&AS, 103, 445

Mathis, J. S., Rumpl, W., & Nordsieck, K. H. 1977, ApJ, 217, 425

Meixner, M., et al. 2006, AJ, 132, 2268

—. 2010, A&A, 518, L71

Moe, M., & De Marco, O. 2006, ApJ, 650, 916

Murakami, H., et al. 2007, PASJ, 59, 369

Perea-Calderón, J. V., García-Hernández, D. A., García-Lario, P., Szczerba, R., & Bobrowsky, M. 2009, A&A, 495, L5

Pollacco, D. L., Hill, P. W., Houziaux, L., & Manfroid, J. 1991, MNRAS, 248, 1P

Prieto, J. L., Sellgren, K., Thompson, T. A., & Kochanek, C. S. 2009, ApJ, 705, 1425

Rao, N. K., & Nandy, K. 1986, MNRAS, 222, 357

Rao, N. K., & Raveendran, A. V. 1993, A&A, 274, 330

Reid, W. A., & Parker, Q. A. 2006a, MNRAS, 365, 401

—. 2006b, MNRAS, 373, 521

Robitaille, T. P., Whitney, B. A., Indebetouw, R., Wood, K., & Denzmore, P. 2006, ApJS, 167, 256

Rodríguez-Gil, P., et al. 2010, MNRAS, 407, L21

Sabogal, B. E., Mennickent, R. E., Pietrzyński, G., & Gieren, W. 2005, MNRAS, 361, 1055

Sargent, B., et al. 2006, ApJ, 645, 395

Sargent, B. A., et al. 2009, ApJ, 690, 1193

Sellgren, K., Werner, M. W., Ingalls, J. G., Smith, J. D. T., Carleton, T. M., & Joblin, C. 2010, ApJ, 722, L54

Sloan, G. C., Kraemer, K. E., Price, S. D., & Shipman, R. F. 2003, ApJS, 147, 379

Sloan, G. C., et al. 2007, ApJ, 664, 1144

Soszyński, I., et al. 2009, Acta Astron., 59, 335

Tisserand, P., et al. 2009, A&A, 501, 985

van Loon, J. T., et al. 2010, AJ, 139, 68

Walker, H. J. 1985, A&A, 152, 58

Waters, L. B. F. M., et al. 1998, A&A, 331, L61

Watson, D. M., et al. 2007, Nature, 448, 1026

Webbink, R. F. 1984, ApJ, 277, 355

Wesson, R., Barlow, M. J., Liu, X., Storey, P. J., Ercolano, B., & de Marco, O. 2008, MNRAS, 383, 1639

Wesson, R., Liu, X., & Barlow, M. J. 2003, MNRAS, 340, 253

Whitney, B. A., Wood, K., Bjorkman, J. E., & Cohen, M. 2003a, ApJ, 598, 1079

Whitney, B. A., Wood, K., Bjorkman, J. E., & Wolff, M. J. 2003b, ApJ, 591, 1049

Young, K., Phillips, T. G., & Knapp, G. R. 1993, ApJ, 409, 725

Zaniewski, A., Clayton, G. C., Welch, D. L., Gordon, K. D., Minniti, D., & Cook, K. H. 2005, AJ, 130, 2293

Zhang, Y., & Kwok, S. 2011, ApJ, 730, 126

Zijlstra, A. A. 2001, in Astrophysics and Space Science Library, Vol. 265, Astrophysics and Space Science Library, ed. R. Szczerba & S. K. Górny, 157
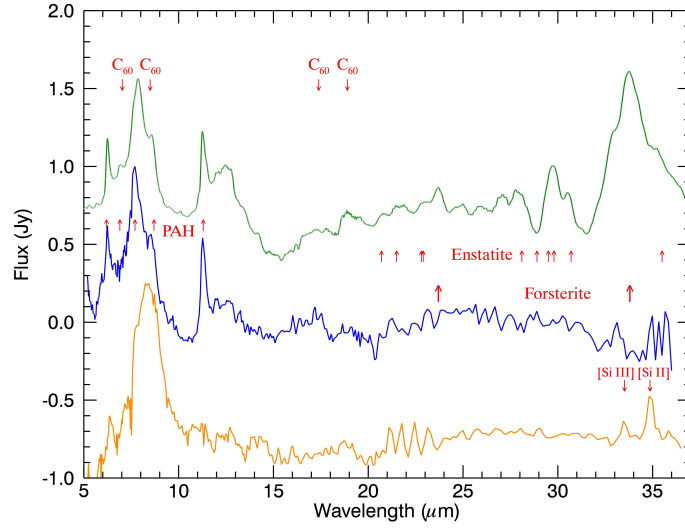
Fig. 1.— Spitzer/IRS spectra of HV 2671 (blue) and V348 Sgr (orange), and the ISO spectrum of CPD –56º 8032 (green). The spectra have been continuum subtracted. CPD –56º 8032 shows emission features attributable to PAHs, crystalline silicates and C_{60}. HV 2671 shows only PAH features. V348 Sgr shows only an unusual feature at ∼8.2 μm.
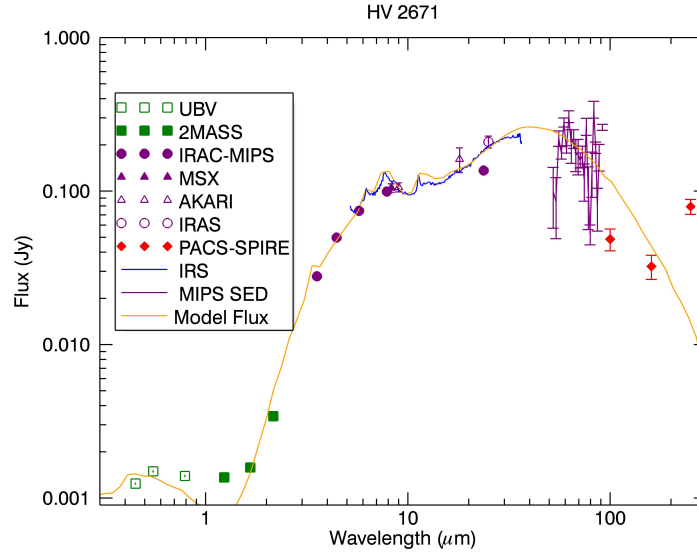
Fig. 2.— SED for HV 2671, and best-fit Monte Carlo RT model. This model consists of amorphous carbon dust in a disk plus a large diffuse envelope. The best fit parameters are shown in Table 4.
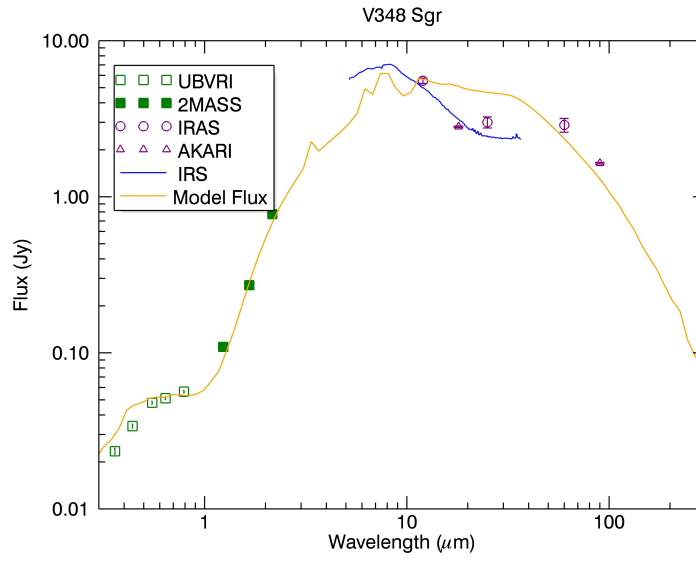
Fig. 3.— SED for V348 Sgr, and best-fit Monte Carlo RT model. This model consists of amorphous carbon dust in a disk plus a large diffuse envelope. The best fit parameters are shown in Table 4. The mismatch seen between the data and the model in the mid-IR may result from the strong emission feature at ∼8.2 μm.
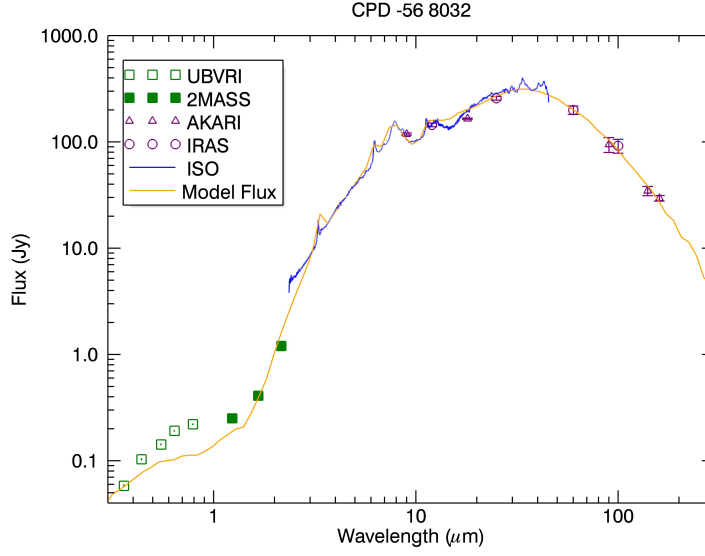
Fig. 4.— SED for CPD –56º 8032, and best-fit Monte Carlo RT model. This model consists of amorphous carbon dust in a disk plus a large diffuse envelope. The best fit parameters are shown in Table 4.
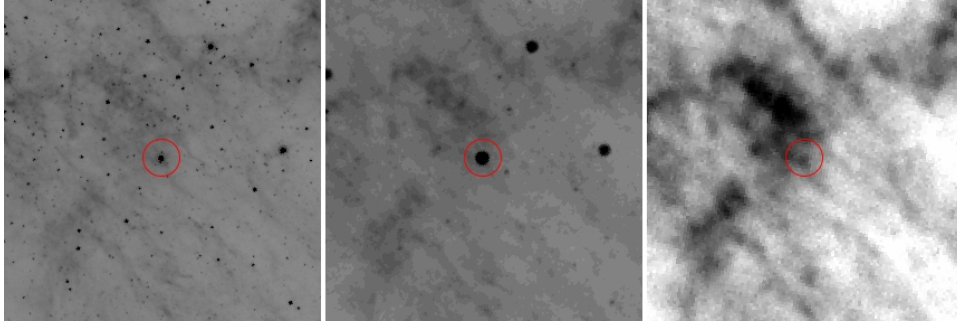

Fig. 5.— Images of HV 2671 in the Spitzer/IRAC 8.0 μm (left), Spitzer/MIPS 24 μm (center), and SPIRE 250 μm (right) bands. The field is $\sim$12′ x 12′.

Table 1.   HV 2671 Photometry

Band	Flux (Jy)[a]
B	1.24e-03 $\pm$ 1.10e-05
V	1.49e-03 $\pm$ 1.40e-05
I_c	1.39e-03 $\pm$ 1.30e-05
2MASS/J	1.36e-03 $\pm$ 4.50e-05
2MASS/H	1.58e-03 $\pm$ 6.20e-05
2MASS/K	3.41e-03 $\pm$ 9.20e-05
IRAC/3.6	2.78e-02 $\pm$ 5.28e-04
IRAC/4.5	4.97e-02 $\pm$ 1.18e-03
IRAC/5.8	7.42e-02 $\pm$ 1.39e-03
IRAC/8.0	9.91e-02 $\pm$ 1.30e-03
MSX/A(8.28)	1.05e-01$\pm$ 6.70e-03
AKARI/9	1.06e-01 $\pm$ 7.23e-03
AKARI/18	1.61e-01 $\pm$ 2.95e-02
MIPS/24	1.36e-01 $\pm$ 6.77e-04
IRAS/25	2.09e-01 $\pm$ 1.88e-02
PACS/100	4.86e-02 $\pm$5.71e-03
PACS/160	3.23e-02 $\pm$ 4.12e-03
SPIRE/250	7.92e-02 $\pm$ 6.21e-03

[a]BVI photometry from Sabogal et al. (2005)

Table 2.   V348 Sgr Photometry

Band	Flux (Jy)[a]
U	2.34e-02 $\pm$ 1.0e-03
B	3.39e-02 $\pm$ 1.0e-03
V	4.78e-02 $\pm$ 1.0e-03
R_c	5.11e-02 $\pm$ 1.0e-03
I_c	5.63e-02 $\pm$ 1.0e-03
2MASS/J	1.09e-01 $\pm$ 2.0e-03
2MASS/H	2.71e-01 $\pm$ 6.0e-03
2MASS/K	7.73e-01 $\pm$ 1.5e-02
AKARI/18	2.81e+00 $\pm$ 2.8e-02
IRAS/12	5.53e+00 $\pm$ 2.2e-01
IRAS/25	3.00e+00 $\pm$ 2.4e-01
IRAS/60	2.88e+00 $\pm$ 2.9e-01
AKARI/90	1.64e+00 $\pm$1.8e-02

[a]UBVRI photometry from Heck et al. (1985)

Table 3.   CPD –56° 8032 Photometry

Band	Flux (Jy)[a]
U	5.80e-02 ± 1.0e-03
B	1.03e-01 ± 1.0e-03
V	1.42e-01 ± 1.0e-03
R_c	1.91e-01 ± 1.0e-03
I_c	2.20e-01 ± 1.0e-03
2MASS/J	2.50e-01± 6.0e-02
2MASS/H	4.08e-01 ± 1.0e-02
2MASS/K	1.20e+00± 3.0e-02
AKARI/9	1.183e+02 ± 2.8e+00
IRAS/12	1.44e+02 ± 5.8e+00
AKARI/18	1.650e+02 ± 2.3e+00
IRAS/25	2.57e+02 ± 1.0e+01
IRAS/60	1.99e+02 ± 1.8e+01
IRAS/100	9.17e+01 ± 1.4e+01
AKARI/90	9.441e+01 ± 1.51e+01
AKARI/140	3.459e+01 ± 3.46e+00
AKARI/160	2.943e+01 ± 1.77e+00

[a]UBVRI photometry from Jones et al. (1999)

Table 4.   Stellar and Dust Parameters

Name	T_{eff}^a (K)	L_{Bol}^b ($L_\odot$)	d^a (kpc)	Disk Mass ($M_\odot$)	Disk Radius[c] (AU)	Envelope Mass ($M_\odot$)	Envelope Radius[c] (AU)	i (deg)
HV 2671	20k	10 900	50	0.07	48/400	5	48/50 000	65
V348 Sgr	20k	6000	5.4	0.05	11/70	1.5×10^{-5}	22/400	<70
CPD–56°8032	34.5k	13 700	1.35	0.08	83/400	1.5	168/23 000	45

[a](De Marco et al. 1997, 2002b)

[b]Bolometric luminosity for the best fit RT models plotted in Figures 2-4.

[c]The two numbers represent the inner and outer radii.